Developmental Cell
Article

Nonautonomous Movement of Chromosomes in Mitosis

Elina Vladimirou,[1,7] Nunu Mchedlishvili,[3,5,7] Ivana Gasic,[3,4,7] Jonathan W. Armond,[2] Catarina P. Samora,[1,6] Patrick Meraldi,[3,4,*] and Andrew D. McAinsh[1,*]
[1]Centre for Mechanochemical Cell Biology, Division of Biomedical Cell Biology, Warwick Medical School
[2]Warwick Systems Biology Center
University of Warwick, Coventry CV4 7AL, UK
[3]Institute of Biochemistry, ETH Zurich, CH-8093 Zurich, Switzerland
[4]Department of Cellular Physiology and Metabolism, Medical Faculty, University of Geneva, CH-1211 Geneva 4, Switzerland
[5]Present address: MRC-LMCB, University College London, London WC1E 6BT, UK
[6]Present address: CRUK London Research Institute, London WC2A 3LY, UK
[7]These authors contributed equally to this work
*Correspondence: patrick.meraldi@unige.ch (P.M.), a.d.mcainsh@warwick.ac.uk (A.D.M.)
http://dx.doi.org/10.1016/j.devcel.2013.08.004

SUMMARY

Kinetochores are the central force-generating machines that move chromosomes during cell division. It is generally assumed that kinetochores move in an autonomous manner. However, we reveal here that movements of neighboring sister-kinetochore pairs in metaphase are correlated in a distance-dependent manner. This correlation increases in the absence of kinetochore oscillations or stable end-on attachments. This suggests that periodic movements of bioriented chromosomes limit the correlated motion of nonsisters. Computer simulations show that these correlated movements can occur when elastic crosslinks are placed between the K-fibers of oscillating kinetochores. Strikingly, inhibition of the microtubule crosslinking motor kinesin-5 Eg5 leads to an increase in nonsister correlation and impairs periodic oscillations. These phenotypes are partially rescued by codepletion of the kinesin-12 Kif15, demonstrating a function for kinesin-5 and kinesin-12 motors in driving chromosome movements, possibly as part of a crosslinking structure that correlates the movements of nonsister kinetochores.

INTRODUCTION

Accurate chromosome segregation during mitosis relies on the capture and alignment of sister chromatids to the spindle equator, and their disjunction into daughter cells by the mitotic spindle. This process requires that sister kinetochores form end-on attachments to bundles of microtubules (K-fibers) emanating from opposite spindle poles. Bioriented sister kinetochores undergo quasiperiodic oscillations along the spindle axis, the exact function of which remains elusive. The prevailing view is that kinetochore-driven chromosome movements are autonomous and largely dependent on kinetochore-mediated control of kinetochore-microtubule plus-end dynamics and forces generated by kinetochore-bound molecular motors (Civelekoglu-Scholey et al., 2013; McIntosh et al., 2012; Skibbens et al., 1993). Nonkinetochore forces, in particular the polar ejection force, which is mediated by plus-end-directed chromokinesins (Funabiki and Murray, 2000; Rieder et al., 1986), and poleward microtubule flux, which is mediated by depolymerization of K-fiber minus ends and microtubule sliding (Matos et al., 2009; Waters et al., 1996), have also been implicated in chromosome movement. Chromokinesins are essential for chromosome alignment in *Xenopus laevis* egg extracts, but they have only a minor effect on kinetochore alignment and oscillations in human somatic cells (Funabiki and Murray, 2000; Stumpff et al., 2012; Wandke et al., 2012). Similarly, in human cells, inactivation of poleward microtubule flux has little effect on chromosome dynamics (Ganem et al., 2005; Jaqaman et al., 2010). Additional mechanical elements within the mitotic spindle, such as the putative microtubule-independent spindle matrices (Qi et al., 2004; Tsai et al., 2006) and lateral connections between K-fibers, could also contribute to the forces acting on chromosomes. The existence of such connections is based on results from electron microscopy, which established that K-fibers may be mechanically linked in anaphase (Nicklas et al., 1982), and laser microsurgery experiments in *Drosophila melanogaster* cells, which revealed that a sister-kinetochore pair does not move when its associated K-fiber is severed (Maiato et al., 2004). However, the molecular nature of these connections and whether they could lead to nonautonomous chromosome movements are unclear.

RESULTS

Human Chromosome Movements in Metaphase Are Nonautonomous

To test whether chromosome movements are autonomous, we recorded HeLa cells stably expressing eGFP-centrin1 (centrosome marker) and eGFP-CENP-A (kinetochore marker) in metaphase using time-lapse fluorescence microscopy and analyzed kinetochore movements using an automated tracking assay (the numbers of all analyzed sister-kinetochore pairs are shown in Table S1 available online; Jaqaman et al., 2010). Upon inspection of sister-kinetochore pair trajectories,

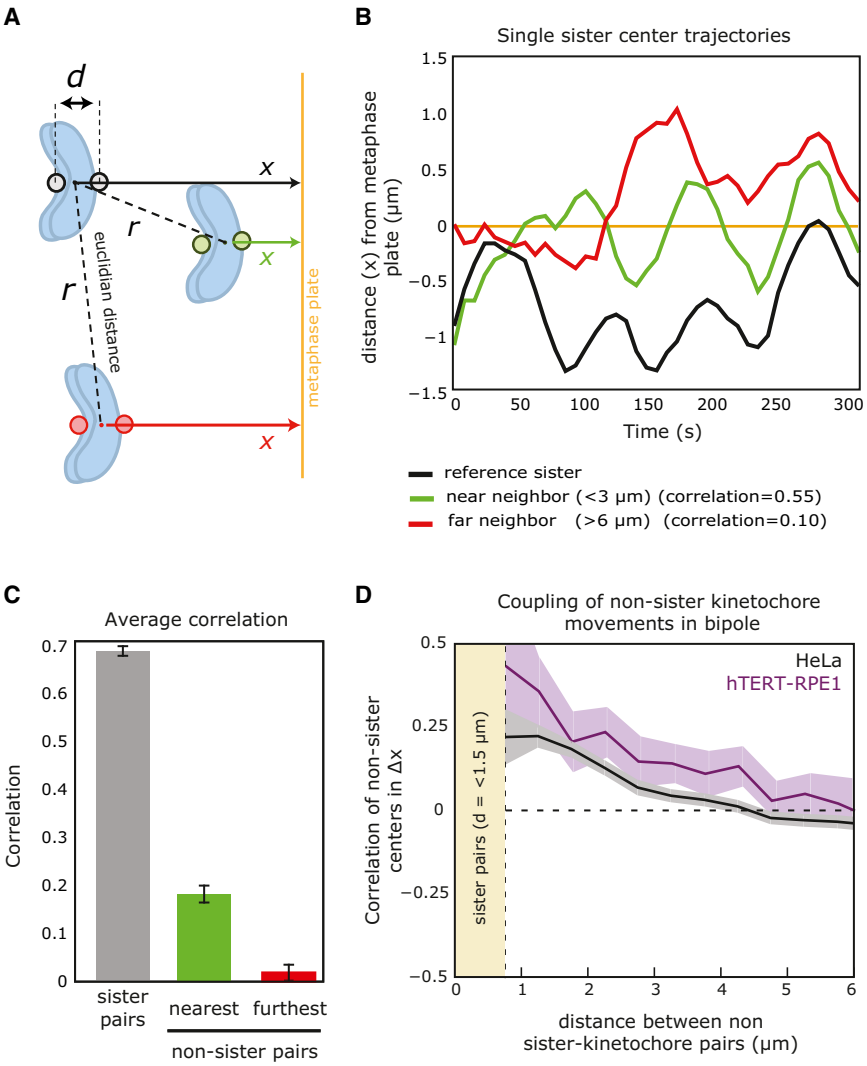

Figure 1. Motion of Nonsister-Kinetochore Pairs Is Coupled in a Distance-Dependent Manner

(A) Schematic of neighboring chromosomes whose sister center position undergoes displacements along the normal (x) to the metaphase plate (orange line) and are positioned *r* μm apart in x, y, z.

(B) Example trajectory (showing the position of the pair in x from the metaphase plate; orange line) of a sister-pair center (black trace) compared with the nearest (green trace) and farthest (red trace) sister-pair center.

(C) Average correlation between sister kinetochore pairs (gray bar), and between the centers of the nearest (minimal *r*; green bar) and farthest (maximal *r*; red bar) neighbors for all nonsister-kinetochore pairs. The numbers of cells and sister kinetochores analyzed for any condition are indicated in Table S1. Error bars represent 95% confidence.

(D) Correlation of nonsister center displacements (Δx) for different values of *r* in HeLa cells (black line) and hTERT-RPE1 eGFP-CENP-A eGFP-centrin 1 cells (purple line). Line thickness represents the 95% confidence. Centers separated by <1.5 μm were excluded from analysis because they are potential sister kinetochores and false positives (marked as yellow zone).

we observed cases in which a given pair showed correlative movement with the nearest, but not the farthest, neighboring sister pair (Figures 1A and 1B). To quantify this, we collected hundreds of sister-kinetochore pair trajectories with a sampling rate of 7.5 s. We then calculated the correlation between sister kinetochore pairs as they moved along the normal to the metaphase plate (Δx). Because we can measure the Euclidian distance between pairs, we can plot the degree of correlation in the entire population as a function of the distance by which they are separated. As a control, we confirmed that the movements of the sister kinetochores, which are physically connected via the centromere, were tightly coupled with an average correlation value of ~0.68 (Figure 1C), which is consistent with our previous study (Jaqaman et al., 2010). The correlation value for the nearest nonsister kinetochore pairs was ~0.22, compared with ~0.02 for the most distant neighbors (Figure 1C). This shows that chromosomes that are close to one another are positively correlated (that is, they tend to move by the same proportion in the same direction). We next plotted the average correlation value as a function of the Euclidian distance between two nonsister-kinetochore pairs. This showed that nonsister-kinetochore pairs are correlated in their movements if they are separated by <3 μm (Figure 1D, gray line). To rule out the possibility that motion correlation of nonsister-kinetochore pairs is specific to aneuploid, transformed HeLa cells, we repeated the experiment in untransformed, diploid retinal epithelial cells (hTERT-RPE1) that express CENP-A-eGFP and eGFP-centrin1 (Magidson et al., 2011). The profile of distance-dependent motion correlation in hTERT-RPE1 cells was similar to that obtained in HeLa cells, showing that it is a general phenomenon (Figure 1D, purple line). We conclude that human chromosomes move nonautonomously in metaphase.

End-On Microtubule Attachments and Kinetochore Oscillations Limit Neighbor Correlation

To test whether this nonautonomous behavior depends on kinetochore-directed movements, we depleted the kinetochore protein Nuf2R, which prevents the formation of normal end-on kinetochore-microtubule attachments (as indicated by a reduction in interkinetochore distances), leaving kinetochores bound to the side of spindle microtubules (Figure 2A; Cai et al., 2009). Such kinetochores display rapid and irregular movements along the microtubules; they are still able to congress to the middle of the spindle, but often fail to remain aligned (Figures 2B–2D). Surprisingly, the correlated motion of such nonsister kinetochores showed a strong increase in comparison with end-on attached kinetochores ($p = 3.7 \times 10^{-42}$, Figure 2E; control depletion did not affect this correlation [see Figure S1 and Table S2]). This

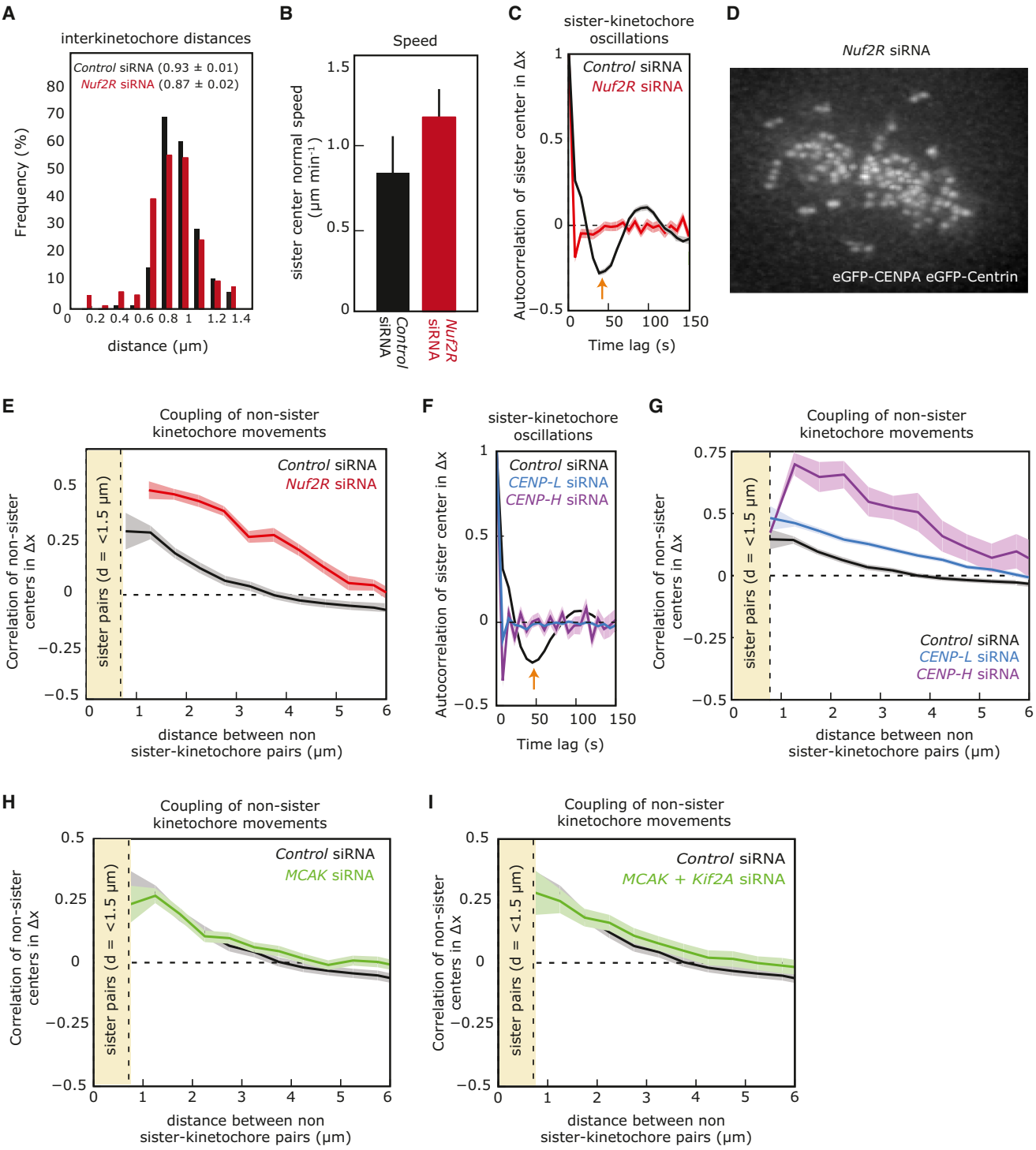

Figure 2. End-On Microtubule Attachments and Irregular Kinetochore Oscillations Limit Neighbor Correlation

(A) Distribution of interkinetochore distances from kinetochore-tracking movies following control (black bars) or *Nuf2R* (red bars) siRNA treatment.

(B) Sister center normal speed (frame-to-frame displacements normal to the metaphase plate) of control or *Nuf2R* siRNA-treated cells. Error bars represent SD.

(C) Autocorrelation of sister-pair center displacements along the normal to the metaphase plate (reveals the periodic nature of chromosome oscillations from a population of trajectories) in control and *Nuf2R* siRNA treated cells. Line thickness represents the 95% confidence interval of the correlations about their mean.

(D) Representative image of a metaphase plate of a *Nuf2R* siRNA-treated cell stably expressing eGFP-CENPA eGFP-Centrin1.

(E) Correlations of nonsister center displacements as a function of the distance between nonsister centers in control siRNA and *Nuf2R* siRNA-treated cells.

(F) Autocorrelation of sister center displacements along the normal to the metaphase plate in control, *CENP-L*, and *CENP-H* siRNA-treated cells. Note that the negative signal at the first time step in *CENP-L* and *CENP-H* siRNA (also *Nuf2R* siRNA in C) indicates random motion (Jaqaman et al., 2010).

(legend continued on next page)

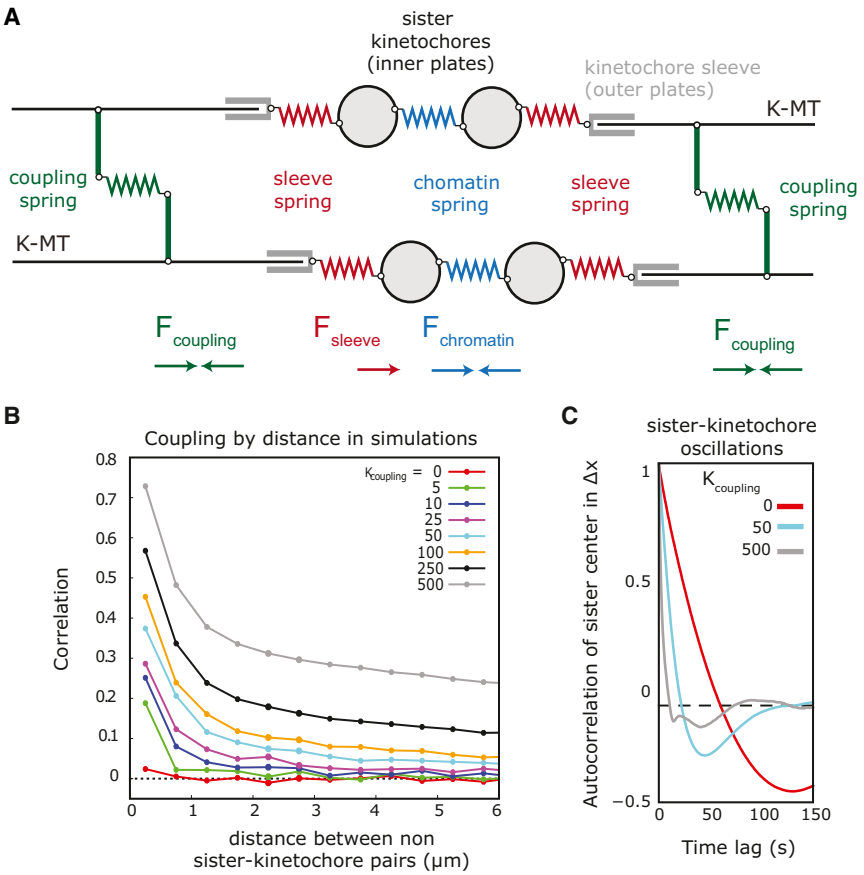

Figure 3. Simulations of Kinetochores with Elastic Linkages Confirm Motion Coupling in a Distance-Dependent Manner

(A) Schematic depiction of the mechanical model used to simulate nearby kinetochores as described in Joglekar and Hunt (2002). Elastic linkages that physically link pairs of K-fibers are shown in green. The direction of forces from coupling spring (green), sleeve spring (red), and chromatin spring (blue) are indicated by colored arrows.

(B) Correlation by distance curves for a range of coupling coefficients $K_{coupling}$.

(C) Correlograms for $K_{coupling}$ = 0 pN $nm^{1/2}$, $K_{coupling}$ = 50 pN $nm^{1/2}$, and $K_{coupling}$ = 500 pN $nm^{1/2}$, showing semiregular oscillations of different periodicity.

indicated that the mitotic spindle itself exerts forces that couple chromosome movements and that the formation of stable end-on kinetochore-microtubule attachments limits this effect. Does this reduction in correlative movements depend only on the formation of end-on attachment, or does it also depend on the typical kinetochore oscillations seen during metaphase? To test this, we reanalyzed sister kinetochore trajectories data from cells that were depleted of CENP-H or CENP-L, two subunits of the CCAN kinetochore complex. The depletion of either CCAN protein does not affect end-on attachments, but is associated with alterations in kinetochore-microtubule dynamics (poleward microtubule flux and the rate of microtubule turnover) and a loss of normal periodic oscillations (Figure 2F; Amaro et al., 2010; Mchedlishvili et al., 2012). Our analysis of the kinetochore trajectories in CENP-H- or CENP-L-depleted cells revealed a strong increase in the correlative movements of nonsister kinetochore pairs ($p = 1.6 \times 10^{-49}$ and 1.3×10^{-20}, respectively; Figure 2G), suggesting that kinetochore oscillations and/or modified kinetochore-microtubule dynamics lead to the changes in the correlation of nonsister movements. To differentiate between these two possibilities, we next depleted the microtubule depolymerase mitotic centromere-associated kinesin (MCAK), which drives microtubule depolymerization at kinetochores, or depleted both MCAK and a second microtubule depolymerase (Kif2a), a condition that abolishes poleward microtubule flux (Ganem et al., 2005; Jaqaman et al., 2010). Consistent with our previous study (Jaqaman et al., 2010), both perturbations modified the period of kinetochore oscillations (Figures S1B and S1C). Moreover, MCAK depletion reduced the speed of kinetochore movements by about 30%, consistent with previous studies (data not shown, but see Jaqaman et al., 2010). However, the correlation of nonsister kinetochore movements was not affected in either condition when compared with control-depleted cells (Figures 2H and 2I). This indicated that nonsister correlation is independent of chromosome oscillation speed/period as well as poleward microtubule flux. Rather, we conclude that the presence of regular oscillatory movements along the spindle axis is sufficient to reduce the correlation of the movements of nonsister kinetochores.

Elastic Crosslinks between K-Fibers Are Sufficient to Generate Neighbor Correlations

What are the mechanisms that could give rise to the correlation of nonsister kinetochore movements? One possibility is physical connections between spindle microtubules. To investigate this idea, we simulated sister kinetochore oscillations using a mathematical model developed from the force-balance model proposed by Joglekar and Hunt (2002) for a single kinetochore pair. The original model was modified to incorporate multiple kinetochore pairs that are randomly distributed within a 10 μm^2 plane that represents the metaphase plate. Simulations of this model produce very regular oscillations of sister kinetochores along the normal to the metaphase plate (Figure 3C). To model

(G) Correlations of nonsister center displacements in control, *CENP-L*, and *CENP-H* siRNA-treated cells.

(H and I) Correlations of nonsister center displacements in control and *MCAK* siRNA-treated cells (H) and control and *MCAK* +*Kif2A* siRNA-treated cells (I). Line thickness represents the 95% confidence interval of the correlations about their mean.

See also Figure S1.

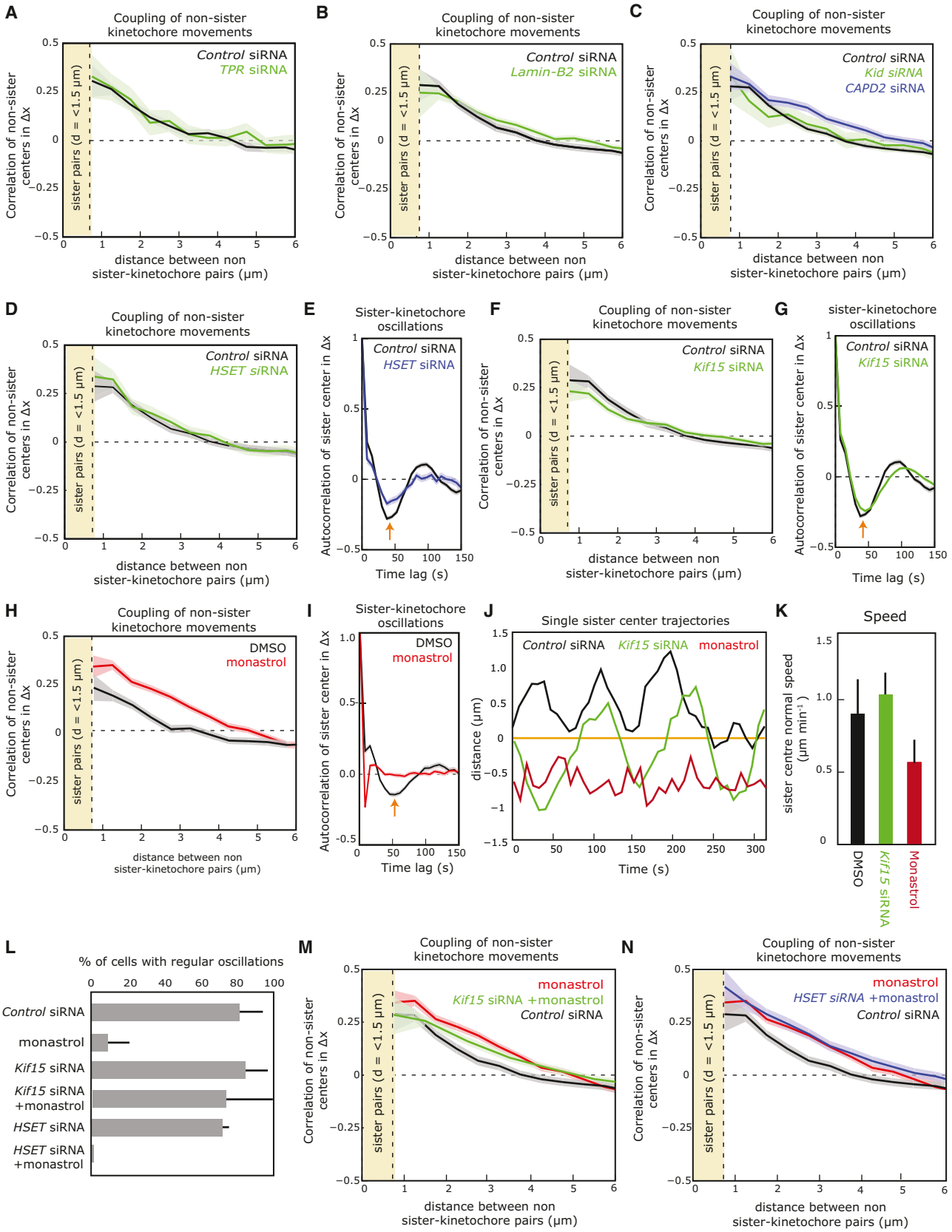

(legend on next page)

physical connections between K-fibers, we added a term to the force balance equations that imposes an elastic linkage between nonsister kinetochore pairs (Figure 3A). The strength of this linkage is given by $K_{coupling}/d^{\alpha}$, where d is the distance between nonsister pairs and α is an exponent that influences the rate at which the linkage strength decays. Thus, a larger α results in the coupling force decaying faster as the distance between nonsister pairs increases. Overall, the elastic linkage acts to reduce the separation of two nonsister kinetochore pairs in the direction normal to the metaphase plate (see schematic in Figure 3A). Simulation of the coupling model using $\alpha = 1.5$ generated distance-dependent correlations between nonsister kinetochore pairs (Figure 3B). As expected, increasing the strength of the coupling force increased the correlations between nonsister pairs. Setting $K_{coupling}$ at ~25 pN $nm^{1/2}$ produced simulations that were in qualitative agreement with experimental data (Figure 3B, magenta line). Importantly, the imposition of this coupling force still allowed sister kinetochores to oscillate (Figure 3C, cyan line). These simulated dynamics more closely reflected real data (Figure 1B), in that they generated more stochastic oscillations compared with the sawtooth-like dynamics generated when the coupling force was removed (Figure 3C, red line). Thus, these simulations show that the presence of inter-K-fiber linkages within the mitotic spindle, with finely tuned physical properties, is sufficient to produce the correlated movements of oscillating sister kinetochore pairs in living cells.

Eg5 and Kif15 Modulate Nonsister Coupling and Kinetochore Oscillations

Our mathematical simulations predict that nonkinetochore elements could connect nonsister kinetochore pairs to produce correlated movements. Such connections could be mediated by a nonmicrotubule spindle matrix, chromosome arms, or a microtubule-dependent structure, which could directly or indirectly connect K-fibers to each other (i.e., molecular motors/microtubule-associated proteins). Depletion of the two most prominent spindle matrix proteins, TPR (the human ortholog of *Drosophila melanogaster* Megator; Qi et al., 2004) and lamin-B2 (Tsai et al., 2006), had no effect on the correlative movements of nonsister kinetochore pairs (Figures 4A and 4B), indicating that they do not contribute to this process. In a second step, we depleted the condensin subunit CAPD2. Such a depletion leads to uncondensed centromeric DNA that decreases the stiffness of the linkage between sister-kinetochores, mechanically uncouples the kinetochore from chromosome arms, and results in a longer oscillation period (Figure S2C; Gerlich et al., 2006; Jaqaman et al., 2010). Here, this depletion led to a weak increase in the correlation of nonsister kinetochore pair movements ($p = 2.2 \times 10^{-11}$; Figure 4C), suggesting that chromosome arms or the stiffness of centromeric DNA contribute to the extent of correlative movements between nonsister kinetochores.

When analyzing the contribution of microtubule-dependent forces, we first depleted the most prominent chromokinesin (Kid; Stumpff et al., 2012) and found no change in correlation of nonsister kinetochore movements, ruling out a role for polar ejection forces (Figure 4C). Second, we tested the contribution of three kinesins that crosslink microtubules (HSET, Kif15, and Eg5). Eg5 is a homotetrameric plus-end-directed motor from the kinesin-5 family that crosslinks parallel microtubules or slides apart antiparallel microtubules, a key process during centrosome separation in early mitosis (Kapitein et al., 2005; Kashina et al., 1996; Sawin et al., 1992). During centrosome separation, Eg5 cooperates with a second plus-end-directed motor (Kif15) from the kinesin-12 family. Current models infer that Kif15 slides apart antiparallel microtubules (Tanenbaum et al., 2009; Vanneste et al., 2009). Eg5 is counterbalanced by HSET, a minus-end-directed motor that also crosslinks and slides apart antiparallel spindle microtubules (Braun et al., 2009; Fink et al., 2009; Hentrich and Surrey, 2010; Mountain et al., 1999). Both HSET and Kif15 were depleted by small interfering RNA (siRNA) treatment, whereas Eg5 was inactivated in metaphase with the small-molecule inhibitor monastrol (Mayer et al., 1999; Eg5 siRNA treatment prior to metaphase results in mitotic cells with monopolar spindles that cannot reach metaphase). HSET depletion did not affect the correlative movements of nonsister kinetochores or more generally the oscillations of sister kinetochores (Figures 4D and 4E). Kif15 depletion also had no effect on kinetochore oscillations, but led to a significant decrease in nonsister correlative movements (Figures 4F and 4G; t test; $p = 2.8 \times 10^{-6}$). In contrast, monastrol-treated cells had an increased correlation in the movements of nonsister kinetochores and lacked the normal oscillatory behavior of kinetochores seen in DMSO-treated cells (Figures 4H–4J; $p = 2.1 \times 10^{-35}$). Kinetochores in monastrol-treated cells also moved 30% more slowly than in control-treated cells (Figure 4K). Treatment with the alternative Eg5 inhibitor

Figure 4. Eg5 and Kif15 Modulate Nonsister Coupling and Kinetochore Oscillations

(A–D) Correlation of nonsister center displacements in control versus *TPR* (A), *Lamin-B2* (B), *Kid* and *CAP-D2* (C), and *HSET* (D) siRNA-treated cells.

(E) Autocorrelation of sister center displacements along the normal to the metaphase plate in control and *HSET* siRNA-treated cells. Orange arrow indicates the half-period.

(F) Correlation of nonsister center displacements in control and *Kif15* siRNA-treated cells.

(G) Autocorrelation of sister center displacements along the normal to the metaphase plate in control and *Kif15* siRNA-treated cells. Orange arrow indicates the half-period.

(H) Correlation of nonsister center displacements in DMSO- and 100 μM monastrol-treated wild-type (WT) cells.

(I) Autocorrelation of sister center displacements along the normal to the metaphase plate in DMSO- and 100 μM monastrol-treated WT cells.

(J) Example trajectories of single sister kinetochore pair centers from control siRNA (black line), *Kif15* siRNA (green line), and monastrol-treated cells (red line).

(K) Sister center normal speed (frame-to-frame displacements normal to the metaphase plate) of DMSO-, *Kif15* siRNA-, and monastrol-treated cells. Error bars represent SD.

(L) Percentage of cells with regular oscillations following control, *Kif15*, or *HSET* siRNA treatment in the presence or absence of monastrol. Oscillations were scored as regular if the correlogram exhibited a negative (nonrandom) trough at approximately −0.2. Error bars represent SD.

(M and N) Correlation of nonsister center displacements in control siRNA versus *Kif15* siRNA or WT cells treated with 100 μM monastrol (M), and in control siRNA versus *HSET* siRNA or WT cells treated with 100 μM monastrol (N).

Line thickness represents the 95% confidence interval of the correlations about their calculated values for (A)–(I), (M), and (N). See also Figure S2 and Table S2.

dimethylenastron (Gartner et al., 2005) had a similar effect, ruling out off-target effects (Figures S2G–S2J). Interestingly, a third inhibitor of Eg5, S-trityl-L-cysteine (STLC) (DeBonis et al., 2004), which is thought to be less potent, also increased the correlation of nonsister-kinetochores movements, and led to oscillations with shorter periods and a lower regularity (Figures S2L and S2M). These data suggest that Eg5 and Kif15, in contrast to their redundant role during centrosome separation, counteract each other in this process (Tanenbaum et al., 2009; Vanneste et al., 2009). To test the latter point, we combined monastrol treatment with Kif15 or HSET depletion. Consistent with previous studies (Tanenbaum et al., 2009), we observed a spindle collapse in half of the cells lacking Kif15 and treated with monastrol (data not shown), which we removed from our analysis. However, in the remaining half that still contained a bipolar spindle, we observed that sister-kinetochores now oscillated along the spindle axis (73% of cells with oscillations compared with 10% of monastrol-treated control cells [Figure 4L]; for analysis of individual cells, see Figure S2N). In contrast, depletion of HSET, which counteracts Eg5 during spindle assembly but does not reduce the correlation in nonsister kinetochore movements, did not rescue the metaphase defects in monastrol-treated cells (Figure 4L). Furthermore, Kif15, but not HSET depletion, partially rescued the high nonsister correlative movement seen in monastrol-treated cells with a bipolar spindle (Figures 4M and 4N). This effect was specific for monastrol treated cells, since Kif15 depletion did not affect the high correlation seen in Nuf2R-depleted cells (Figure S2O). Conversely, treating CENP-L-depleted cells with monastrol did not have an additive effect on neighbor coupling (Figure S2P). This would suggest that motors only affects neighbor coupling when sister kinetochore are bioriented and oscillating.

Nonkinetochore Activities Regulate Chromosome Movements

The above data suggested that Eg5 and Kif15 are part of the lateral connections between K-fibers predicted by our simulations that would regulate the correlative movements of nonsister kinetochores. Consistent with this hypothesis and previous reports (Ma et al., 2011), we confirmed that both the Eg5 and Kif15 motors bind K-fibers in cold-treated cells, a condition that depolymerizes all nonkinetochore microtubules (Figure 5A). Alternatively, one could also imagine that Eg5 inhibition directly impairs the ability of kinetochores to generate directional movements. Indeed, the budding yeast kinesin-5 Cin8 has been implicated in the regulation of kinetochore-microtubule dynamics (Gardner et al., 2008). To rule out direct effects of Eg5 on kinetochore function, we investigated the attachment status of kinetochores and their ability to regulate kinetochore-microtubule dynamics. We did not observe enrichment of the spindle checkpoint protein Mad1 on kinetochores (a marker of unattached kinetochores) or changes in interkinetochore distances (a measure of force applied across sisters), indicating that bioriented attachments and force generation at kinetochores were normal (Figures 5B and 5C). We also found no significant changes in interpolar distances, arguing against a compression of the mitotic spindle (Figure 5D). To test whether monastrol affected microtubule dynamics in human cells, we used a HeLa cell line expressing photoactivatable GFP-α-tubulin to measure turnover of kinetochore-microtubule and poleward microtubule flux, and HeLa cells expressing EB3-tdTomato, a marker for growing microtubule plus ends (Amaro et al., 2010; Samora et al., 2011). Because the turnover rate of kinetochore-microtubules and the rate of poleward flux (consistent with previous studies; Cameron et al., 2006) and microtubule growth speeds were unaffected in monastrol-treated cells when compared with control treatment (Figures 5E–5I), we concluded that Eg5 inhibition does not impair the dynamic instability of kinetochore-microtubules. This would suggest that Eg5 affects chromosome movements through an unknown mechanism, possibly through its capacity to crosslink, directly or indirectly, K-fibers. Consistent with such a hypothesis, our mathematical simulations showed that an increase in the coupling constant $K_{coupling}$ led to progressively shorter oscillation periods and a loss of regularity, similar to the phenotype seen in STLC-, dimethylenastron-, or monastrol-treated cells (Figures 3C and S2).

To more directly test for this possibility, we took advantage of a small-molecule inhibitor of Eg5 (FCPT) that locks the motor into a tightly bound (rigor) state, as opposed to monastrol, which traps Eg5 in a low-friction mode (Crevel et al., 2004; Groen et al., 2008). Treatment of cells with FCPT, as with monastrol, abolished regular kinetochore oscillations and increased nonsister coupling without impairing the dynamic instability of spindle microtubules, as visualized with a HeLa cell line expressing EB3-tdTomato (Figures 6A and 6B; Movies S1 [control] and S2 [FCPT treated]). By staining FCPT-treated cells with antibodies against α-tubulin, we could observe thick bundles of K-fibers that appeared to connect kinetochores to the spindle poles (Figure 6C). To confirm this initial finding, we also cold treated cells to remove nonkinetochore microtubules and stained them with anti-α-tubulin and Eg5 antibodies. These immunofluorescence experiments revealed a drastic reorganization of K-fiber architecture. Whereas control-treated cells contained many individual K-fibers, FCPT-treated cells contained only a few bright K-fibers, which often branched out (Figure 6C). Strikingly, Eg5 was present on these thick bundles of K-fibers up to the branching point, but was absent on individual K-fibers. Based on these results, we conclude that Eg5 has the ability to crosslink neighboring K-fibers in metaphase.

DISCUSSION

Our data demonstrate that chromosome movements are not autonomous during mitosis in human cells, as we quantitatively demonstrate that nonsister kinetochores' movements are correlated when they are in close proximity. We term this behavior neighbor coupling. Our mathematical simulations suggest that neighbor coupling can arise if kinetochore fibers are physically connected, allowing transmission of force. This model recapitulates the partially stochastic nature of chromosome oscillations seen in vivo, and postulates the existence of nonkinetochore-bound factors within the spindle that have a profound influence on chromosome movements. The distance-dependent nature of the neighbor coupling, and the fact that it does not lead to the entire spindle locking together, suggests that these connections operate over short timescales. We therefore suggest

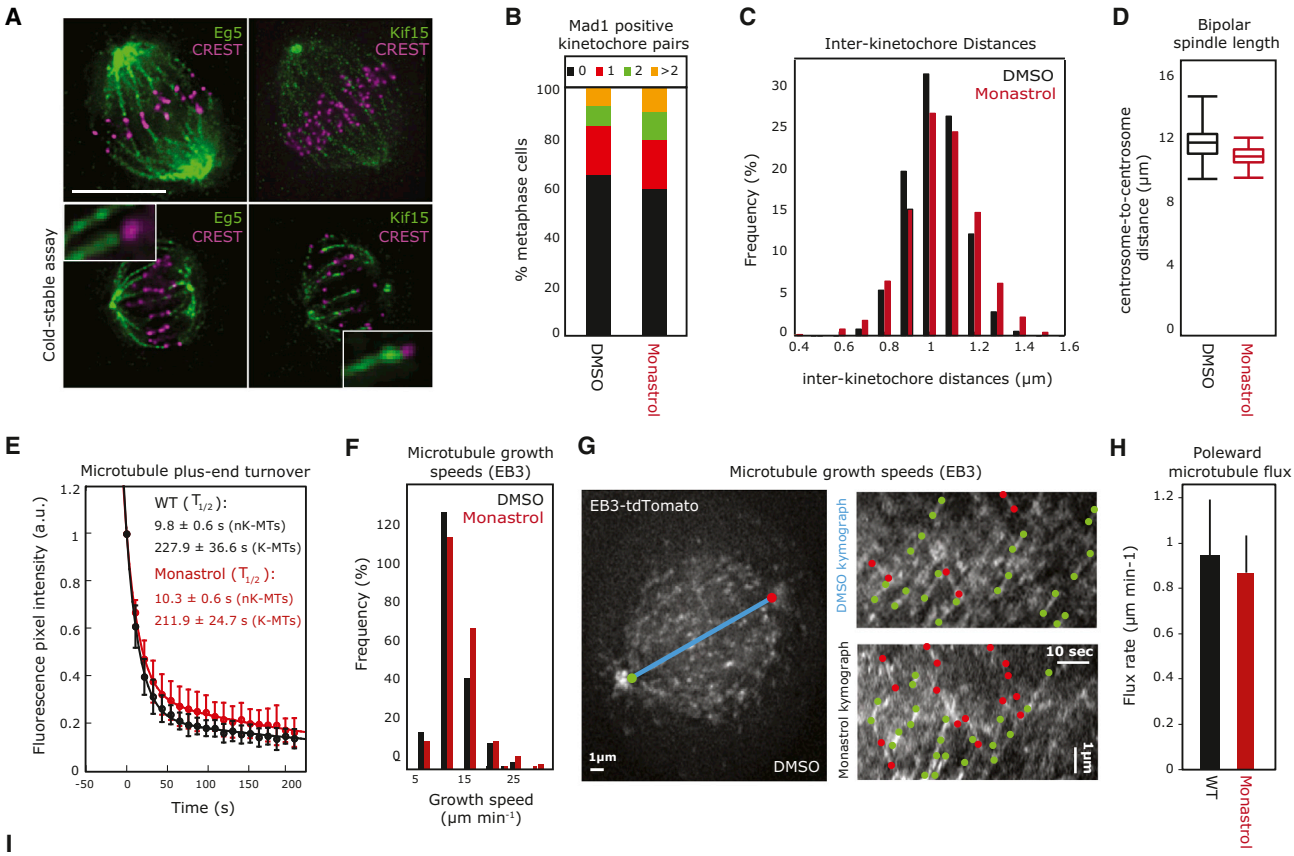

Figure 5. Eg5 Is Required for Normal Sister-Kinetochore Movements in Metaphase

(A) Images of cells stained with antibodies against Eg5 or Kif15 (green) and CREST (magenta). Lower row shows cells treated with ice-cold medium to depolymerize nonkinetochore microtubules.

(B) Cells were treated with DMSO or 100 μM monastrol, fixed for immunofluorescence, and stained with anti-Mad1 antibodies. Metaphase cells were classified as containing zero, one, two, or more than two Mad1-positive kinetochore pairs. The graph represents three independent experiments with >100 cells per experiment.

(C) Distribution of intersister kinetochore distances from kinetochore-tracking movies following DMSO or 100 μM monastrol treatment.

(D) Box plot of centrosome-to-centrosome distances of bipolar spindles following DMSO or 100 μM monastrol treatment.

(E) Quantification of fluorescence intensity decay of photoactivated (PA)-GFP-α-tubulin regions over time as seen in (I). Using a double exponential decay function, the corresponding half-lives of the fast (P_f) and slow (P_s) microtubule populations in cells treated with either DMSO or 100 μM monastrol were calculated. Error bars represent SEM.

(F) Microtubule growth speeds in cells expressing EB3-tdTomato following DMSO or 100 μM monastrol treatment.

(G) Example frame from a movie (single z section, every 1 s for 1 min) of EB3-tdTomato expressing cells (green and red dots in left panel indicate location of spindle poles). Kymographs (see right panels) were constructed along the spindle axis (blue line). Colored dots mark the start and end of EB3 movements which were used to calculate speeds (plotted in F) from DMSO-and monastrol-treated cells. Red and green designate the pole from which an EB comet originates.

(H) Quantification of poleward microtubule flux rates. Error bars represent SD.

(I) Successive frames acquired every 30 s before and after photoactivation of stable PA-GFP-α-tubulin/Histone2B-mRFP HeLa cells treated as indicated. Green arrowheads mark the initial position of the PA spot. The decay of the signal allowed us to calculate the turnover of the microtubule populations as shown in (E). Displacement of PA spot over time gives speed of poleward microtubule flux (plotted in H). Scale bar, 6 μm.

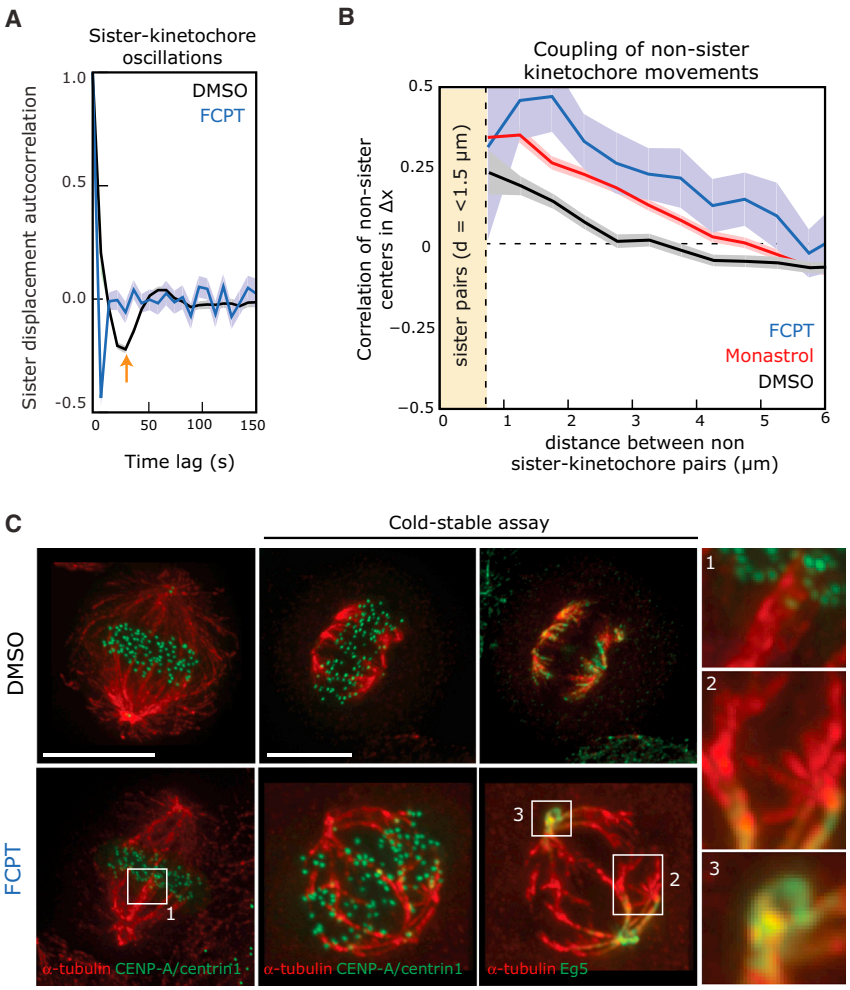

Figure 6. The Eg5 Inhibitor FCPT Bundles K-Fibers

(A) Autocorrelation of sister center displacements along the normal to the metaphase plate in DMSO- and FCPT-treated cells.

(B) Correlation of nonsister center displacements in DMSO-, 100 μM monastrol-, and FCPT-treated cells.

(C) HeLa eGFP-CENPA eGFP-Centrin1 were treated with DMSO or FCPT, subjected to cold treatment or not, and stained with antibodies against α-tubulin and Eg5. The first column shows the α-tubulin (red) and the GFP signal (green) in non-cold-treated cells, the second column shows cold-treated cells with the α-tubulin (red) and the GFP signal (green), and the third column shows the same cold-treated cell with the Eg5 signal (green) and the α-tubulin (red) signal. Zoomed regions show bundled K-fibers in noncold, FCPT-treated cells (1); branching K-fibers in cold-treated FCPT cells (2); and the localization of Eg5 to poles in the presence of FCPT (3). Scale bars, 5 μm. See also Movies S1 and S2.

that connections impose a bias on the direction of the kinetochore and hence the chromosome movements. These findings are consistent with previous studies that proposed that chromosomes are glued together through chromosome arms or lateral association of kinetochore-microtubules (Chaly and Brown, 1988; Maiato et al., 2004; Nicklas and Arana, 1992).

Our study identifies the nonkinetochore-bound plus-end-directed kinesins Eg5 and Kif15, which play an essential but additive role during centrosome separation and maintenance of spindle bipolarity (Tanenbaum et al., 2009; Vanneste et al., 2009), as key potential regulators of neighbor coupling and chromosome movements. Inhibition of Eg5 leads to loss of chromosome oscillations in metaphase, a phenotype that is rescued by the depletion of Kif15. Given that Kif15 depletion is the only condition that reduced the correlation of nonsister kinetochore movements, and that our FCPT experiments indicate that Eg5 has the ability to crosslink K-fibers, we postulate that Kif15 acts as a mechanical coupling factor in metaphase that is limited in its action by Eg5. The known biophysical properties of each motor would suggest that the plus-end stepping action of these two kinesins (Boleti et al., 1996; Cole et al., 1994; Sawin et al., 1992) and potentially the extensile sliding of antiparallel microtubules (Tanenbaum et al., 2009; Vanneste et al., 2009) are involved in this process. One possibility is that Eg5 normally exerts drag in the system and limits force generation by Kif15. Consistent with this idea, a previous in vitro experiment showed that Eg5 slows down microtubule sliding driven by kinesin-1 (Crevel et al., 2004). This drag component could also be relieved by addition of monastrol, which traps the motor in the weak-bound ADP-state (Crevel et al., 2004). This counteracting relationship is consistent with recent work showing that Kif15 modulates K-fiber-generated forces that oppose Eg5-generated forces (Sturgill and Ohi, 2013). That work and our own study stand in contrast to the redundant role of Eg5 and Kif15 in maintaining spindle bipolarity (Tanenbaum et al., 2009; Vanneste et al., 2009). However, we cannot rule out the possibility that Eg5-monastrol complexes, which remain bound to the spindle, increase neighbor coupling by increasing spindle viscosity. A prediction of this model is that loss of the motor would actually lower coupling. It would also be interesting to determine how modifying Eg5/Kif15 would affect the viscosity and elasticity of the human mitotic spindle (Shimamoto et al., 2011).

Whether the function of Eg5 reflects the previously reported static pool of Eg5 in *Xenopus* (Kapoor and Mitchison, 2001) is an open question. Furthermore, the bulk population of Eg5 motors is preferentially localized on microtubules close to the poles, whereas Kif15 motors are uniformly present on all spindle microtubules, including K-fibers (this study and Sturgill and Ohi, 2013). It is possible that these differential localization patterns of each motor can explain the motors' additive role in controlling spindle bipolarity and their counteracting relationship in controlling chromosome dynamics. Finally, our results already suggest that multiple factors beyond Kif15 and Eg5 must be involved in the mechanical coupling of chromosome movements, because Kif15 depletion does not abolish neighbor coupling. In particular,

the results we obtained following depletion of Nuf2R and CAPD2 suggest that steric hindrance of chromosome arms as well as the mitotic spindle itself (e.g., the viscoelastic properties of the microtubule network) can give rise to forces that couple the movements of chromosomes over short time periods. Indeed, any viscous medium theoretically can contribute to neighbor coupling (see, e.g., Binous and Phillips, 1999). We further note that stabilization of K-fibers (by CENP-H depletion; Amaro et al., 2010) or bundling of K-fibers (by FCPT treatment) leads to particularly high levels of neighbor coupling, arguing for a key role of K-fibers in this phenomenon. Therefore, we predict that short of getting rid of the entire mitotic spindle, it would be impossible to abolish neighbor coupling in mitosis.

How does the inhibition of Eg5 by monastrol lead to high coupling and a loss of oscillations? Our results demonstrate that Eg5 does not affect chromosome movements in metaphase through control of kinetochore-microtubule dynamics. It is tempting to speculate that an increase in neighbor coupling would be sufficient to block chromosome oscillations, since our mathematical simulations show that an increase in the $K_{coupling}$ first leads to a shortening of the oscillation period, as seen in STLC-treated cells, and beyond a threshold value results in abolishment of oscillations and increase in neighboring coupling, which is in qualitative agreement with our monastrol data (Figure 3C). However, loss of oscillations per se also leads to a high neighbor coupling, as seen in CENP-H or CENP-L-depleted cells. It is possible that the imposition of periodic oscillations during metaphase reduces neighbor coupling, thereby preventing the interlocking of chromosome arms, or forces derived from the viscoelastic properties of the spindle. This ''decoupling'' mechanism has parallels with oscillations of the nucleus during meiotic prophase in fission yeast, which are thought to aid the search for homology by resolving the interlocking of homologous chromosomes (Chikashige et al., 1994; Yamamoto et al., 1999). Nevertheless, at this stage, it is not possible to formally state the causality between oscillations and neighbor coupling.

In conclusion, our data show that nonkinetochore localized motor proteins play a crucial role in normal chromosome movement in human cells. These chromosome movements are also not autonomous, being influenced by the movement state of their neighbors. Thus, the overall dynamics of chromosomes in mitosis cannot be understood through a mechanistic understanding of kinetochore function alone. This conclusion is consistent with recent studies indicating the importance of the spatial organization of chromosomes in the spindle for timely chromosome congression in human cells and mouse oocytes (Kitajima et al., 2011; Magidson et al., 2011). A major challenge will be to develop a mathematical framework to understand how multiple kinetochore and nonkinetochore forces are integrated within the spindle over various timescales to give rise to the observed microscopic movements of chromosomes during mitosis.

EXPERIMENTAL PROCEDURES

Cell Culture and Drug and siRNA Treatments

HeLa eGFP-CENP-A/eGFP-centrin1, HeLa eGFP-CENP-A, HeLa eGFP-CENP-A/EB3-tdTomato (MC049), and hTERT-RPE1 eGFP-CENP-A/eGFP-centrin1 cells (a kind gift from A. Khodjakov; Magidson et al., 2011) were grown in Dulbecco's modified medium (DMEM) containing 10% fetal calf serum (FCS), 100 U/ml penicillin, and 100 mg/ml streptomycin at 37°C with 5% CO_2. Live-cell imaging experiments were performed at 37°C in Lab-Tek II chambers (Thermo Fisher Scientific) with Leibovitz L-15 medium containing 10% FCS. siRNA oligonucleotides were transfected as indicated in the Supplemental Experimental Procedures. For drug treatments, cells were treated with 10 μM dimethylenastron (Calbiochem), 100 μM monastrol (Tocris Bioscience), or 100 μM FCPT (a kind gift from T. Mitchison) for 30 min before live-cell imaging analysis or fixed-cell imaging. STLC (40 μM; Sigma) was added for 1 hr in the presence of the proteasome inhibitor MG132 (1 μM; Sigma), due to its slower uptake. Fixed imaging was carried out as indicated in the Supplemental Experimental Procedures.

Live-Cell Imaging, Photoactivation, and EB3 Dynamics Experiments

Live-cell imaging of HeLa eGFP-CENP-A eGFP-centrin1 cells for kinetochore tracking was carried out as previously described (Jaqaman et al., 2010; see Supplemental Experimental Procedures for further details). Photoactivation experiments were performed on bipolar metaphase spindles as previously described (Amaro et al., 2010). The microtubule growth speeds were measured in cells expressing eGFP-CENP-A/EB3-tdTomato after a 30 min treatment with monastrol or DMSO. Images (512 × 512) were acquired at 50% neutral density, 300 ms exposure, and a temporal resolution of 500 ms for 120 s using a tetramethylrhodamine isothiocyanate (TRITC) filter set. Images were deconvolved with medium noise filtering for eight iterations using SoftWorx. The speeds of EB3 comets were measured using an ImageJ kymograph plugin (http://www.embl.de/eamnet/html/body_kymograph.html).

Statistical Analysis of Kinetochore Dynamics

Kinetochore tracking was carried out as previously described (Jaqaman et al., 2010). To analyze the behavior of CENP-L- and CENP-H-depleted cells, we reanalyzed kinetochore trajectories previously recorded in our laboratory (Amaro et al., 2010; Mchedlishvili et al., 2012). The statistical analysis of kinetochore dynamics was performed with CupL, a custom MATLAB software for analyzing kinetochore tracking data. The data were filtered such that only tracks that were at least 75% complete and cells with at least two pairs of tracks were included in the analysis. The kinetochore speeds along the metaphase plate normal axis were calculated as the absolute displacement along the normal axis divided by the time interval, averaged across the track length and then across cells for each condition. Autocorrelation of sister center displacements (Δx) is defined for t = 0,1,2,...,n, and time lags τ = 0,1,2,...,n-1 are defined as

$$A(\tau) = \frac{1}{\sigma^2}\langle(\Delta x(t+\tau) - \mu)(\Delta x(t) - \mu)\rangle$$

where $\Delta x(t)$ is the displacement normal to the metaphase plate of the sister-kinetochore center at time t, μ is the mean of $\Delta x(t)$, σ is the SD of $\Delta x(t)$, and $\langle\ \rangle$ indicates ensemble averaging. For each condition, $A(\tau)$ was calculated for every track and then averaged. The correlation function is defined for t = 0,1,2,...n as

$$C(\tau) = \frac{1}{\sigma_x \sigma_y}\langle(\Delta x(t+\tau) - \mu_x)(\Delta y(t) - \mu_y)\rangle$$

where the time lag τ = 0,1,2,...,n-1, μ_x and μ_y are the means of $\Delta x(t)$ and $\Delta y(t)$, σ_x and σ_y are the SDs of $\Delta x(t)$ and $\Delta y(t)$, and $\langle\ \rangle$ indicates ensemble averaging. $C(\tau)$ was calculated for each sister-kinetochore pair against its nearest and farthest neighbors and then averaged. To calculate the correlation of nonsister pairs with respect to their separation in space, the correlation at time lag $\tau = 0$, $C(0)$ was calculated for each possible combination of sister-kinetochore pair center displacements within a cell. The distance between tracks was calculated as the Euclidean distance between the average position of the kinetochore pair centers. The correlation values were then binned by distance into 0.5 μm bins, and the mean and SEM were calculated.

We estimated the 95% confidence intervals of the correlations about their calculated values as $\pm 2\sigma/\sqrt{n}$, where σ is the SD and n is the number of observations.

Hypothesis Testing of Correlation Values across Conditions

The significance of nonsister kinetochore coupling was tested via t test (assuming equal variances) on the correlation values of nonsister kinetochore pairs that were no more than 3 μm apart.

Simulations

Simulations of nonsister kinetochore pair coupling were performed using a modification of the model proposed by Joglekar and Hunt (2002). First, we extended the model to account for m independent kinetochore pairs. We then postulated a spring force that tended to reduce the separation of two nonsister kinetochore pairs in the direction normal to the metaphase plate. We imposed this force pairwise between each nonsister kinetochore pair, and furthermore varied the strength of the force inversely with distance between pairs in the metaphase plate plane. The force balance equation of the model of Joglekar and Hunt was modified to

$$\text{Left Kinetochore Forces} + \text{Left Kinetochore Coupling Forces} + \text{Right Ejection Forces} = \text{Right Kinetochore Forces} + \text{Right Kinetochore Coupling Forces} + \text{Left Ejection Forces}$$

Writing in terms of kinetochore positions, we find two linear simultaneous equations for each kinetochore i

$$K_{\text{sleeve}} \sum_{j=1}^{n} \left(X_i^L - S_{ij}^L \right) - K_{\text{coupling}} \sum_{\substack{j=1 \\ j \neq i}}^{m} \frac{X_j^C - X_i^C}{D_{ij}^{\alpha}} - F_{\text{PE}}\left(X_i^C \right) = K_{\text{kinet}} \left(X_i^R - X_i^L - \gamma \right) \quad (1)$$

$$K_{\text{sleeve}} \sum_{j=1}^{n} \left(S_{ij}^R - X_i^R \right) + K_{\text{coupling}} \sum_{\substack{j=1 \\ j \neq i}}^{m} \frac{X_j^C - X_i^C}{D_{ij}^{\alpha}} + F_{\text{PE}}\left(X_i^C \right) = K_{\text{kinet}} \left(X_i^R - X_i^L - \gamma \right) \quad (2)$$

where X_i^L, X_i^R, and X_i^C are the left kinetochore, right kinetochore, and center position, respectively, of the kinetochore pair i. S_{ij}^L and S_{ij}^R are the positions of the sleeve for the j^{th} microtubule on the i^{th} left and right kinetochores, respectively. K_{sleeve}, $K_{coupling}$, and K_{kinet} are the sleeve, nonsister kinetochore pair coupling, and sister-kinetochore spring constants, respectively. D_{ij}^{α} is the α^{th} power of the distance between kinetochore pairs in the metaphase plate plane. $F_{\text{PE}}(\bullet)$ is the polar ejection force function, as described in Joglekar and Hunt (2002), and γ is the rest length of the sister-kinetochore spring.

The solution of these equations for X_i^L and X_i^R is used to iteratively update the positions of the kinetochores, using the positions in the previous time step to evaluate X_i^C. Kinetochore pairs were positioned on a 10 μm square using Sobol quasirandom numbers in two dimensions (Press et al., 2007). Pairs were fixed in the metaphase plate plane (y and z coordinates) and only allowed to move normal to the plate.

The rest of the simulation code and parameters were equivalent to those in Joglekar and Hunt (2002) and run on MATLAB 2013a. For each set of parameter values, we performed 48 independent simulations of 40 kinetochore pairs for 600 s (600,000 iterations, with 50,000 "burn-in" iterations discarded to allow stabilization) to calculate error estimates.

SUPPLEMENTAL INFORMATION

Supplemental Information includes Supplemental Experimental Procedures, two figures, two tables, and two movies and can be found with this article online at http://dx.doi.org/10.1016/j.devcel.2013.08.004.

ACKNOWLEDGMENTS

We thank the LMC for microscopy support, D. Gerlich for CAP-D2 siRNA, and U. Kutay for lamin-B2 siRNA/antibodies (all ETHZ); I. Vernos (CRG Barcelona) for Kif15 antibodies; and A. Khodjakov (Wadsworth Center) for hTERT-RPE1 eGFP-CENP-A cells. We thank H. Maiato (ICMB), S. Dumont (Harvard), and M. Mishima and N. Burroughs (University of Warwick) for critical input. Work in the Meraldi group was supported by the SNF-Förderungprofessur, the ETHZ, the University of Geneva, and the Louis-Jeantet Foundation. I.G. and N.M. were supported by Böhringer Ingelheim fellowships and are part of the MLS PhD school. Work in the McAinsh group was supported by Marie Curie Cancer Care and the BBSRC (BB/I021353/1). This project was codirected by A.D.M and P.M. and initiated, planned, and conceived by E.V., N.M., P.M., and A.D.M. Data interpretation was carried out by N.M., E.V., I.G., P.M., and A.D.M. E.V., N.M., and I.G. contributed equally to the experiments, with the exception of the development of computational tools, which was done by E.V. J.W.A. and E.V. established the simulations, and C.S. and E.V. performed the photoactivation experiments. The manuscript was prepared by A.D.M. and P.M. with contributions from E.V., N.M., and I.G.

Received: February 21, 2013
Revised: June 17, 2013
Accepted: August 5, 2013
Published: October 14, 2013

REFERENCES

Amaro, A.C., Samora, C.P., Holtackers, R., Wang, E., Kingston, I.J., Alonso, M.C., Lampson, M.A., McAinsh, A.D., and Meraldi, P. (2010). Molecular control of kinetochore-microtubule dynamics and chromosome oscillations. Nat. Cell Biol. *12*, 319–329.

Binous, H., and Phillips, R.J. (1999). Dynamic simulation of one and two particles sedimenting in viscoelastic suspensions of FENE dumbbells. J. Non-Newt. Fluid Mech. *83*, 93–130.

Boleti, H., Karsenti, E., and Vernos, I. (1996). Xklp2, a novel Xenopus centrosomal kinesin-like protein required for centrosome separation during mitosis. Cell *84*, 49–59.

Braun, M., Drummond, D.R., Cross, R.A., and McAinsh, A.D. (2009). The kinesin-14 Klp2 organizes microtubules into parallel bundles by an ATP-dependent sorting mechanism. Nat. Cell Biol. *11*, 724–730.

Cai, S., O'Connell, C.B., Khodjakov, A.L., and Walczak, C.E. (2009). Chromosome congression in the absence of kinetochore fibres. Nat. Cell Biol. *11*, 832–838.

Cameron, L.A., Yang, G., Cimini, D., Canman, J.C., Kisurina-Evgenieva, O., Khodjakov, A.L., Danuser, G., and Salmon, E.D. (2006). Kinesin 5-independent poleward flux of kinetochore microtubules in PtK1 cells. J. Cell Biol. *173*, 173–179.

Chaly, N., and Brown, D.L. (1988). The prometaphase configuration and chromosome order in early mitosis. J. Cell Sci. *91*, 325–335.

Chikashige, Y., Ding, D.Q., Funabiki, H., Haraguchi, T., Mashiko, S., Yanagida, M., and Hiraoka, Y. (1994). Telomere-led premeiotic chromosome movement in fission yeast. Science *264*, 270–273.

Civelekoglu-Scholey, G., He, B., Shen, M., Wan, X., Roscioli, E., Bowden, B., and Cimini, D. (2013). Dynamic bonds and polar ejection force distribution explain kinetochore oscillations in PtK1 cells. J. Cell Biol. *201*, 577–593.

Cole, D.G., Saxton, W.M., Sheehan, K.B., and Scholey, J.M. (1994). A "slow" homotetrameric kinesin-related motor protein purified from Drosophila embryos. J. Biol. Chem. *269*, 22913–22916.

Crevel, I.M.-T.C., Alonso, M.C., and Cross, R.A. (2004). Monastrol stabilises an attached low-friction mode of Eg5. Curr. Biol. *14*, R411–R412.

DeBonis, S., Skoufias, D.A., Lebeau, L., Lopez, R., Robin, G., Margolis, R.L., Wade, R.H., and Kozielski, F. (2004). In vitro screening for inhibitors of the human mitotic kinesin Eg5 with antimitotic and antitumor activities. Mol. Cancer Ther. *3*, 1079–1090.

Fink, G., Hajdo, L., Skowronek, K.J., Reuther, C., Kasprzak, A.A., and Diez, S. (2009). The mitotic kinesin-14 Ncd drives directional microtubule-microtubule sliding. Nat. Cell Biol. *11*, 717–723.

Funabiki, H., and Murray, A.W. (2000). The Xenopus chromokinesin Xkid is essential for metaphase chromosome alignment and must be degraded to allow anaphase chromosome movement. Cell *102*, 411–424.

Ganem, N.J., Upton, K., and Compton, D.A. (2005). Efficient mitosis in human cells lacking poleward microtubule flux. Curr. Biol. *15*, 1827–1832.

Gardner, M.K., Bouck, D.C., Paliulis, L.V., Meehl, J.B., O'Toole, E.T., Haase, J., Soubry, A., Joglekar, A.P., Winey, M., Salmon, E.D., et al. (2008). Chromosome congression by Kinesin-5 motor-mediated disassembly of longer kinetochore microtubules. Cell *135*, 894–906.

Gartner, M., Sunder-Plassmann, N., Seiler, J., Utz, M., Vernos, I., Surrey, T., and Giannis, A. (2005). Development and biological evaluation of potent and specific inhibitors of mitotic Kinesin Eg5. ChemBioChem *6*, 1173–1177.

Gerlich, D.W., Hirota, T., Koch, B., Peters, J.-M., and Ellenberg, J. (2006). Condensin I stabilizes chromosomes mechanically through a dynamic interaction in live cells. Curr. Biol. *16*, 333–344.

Groen, A.C., Needleman, D.J., Brangwynne, C.P., Gradinaru, C., Fowler, B., Mazitschek, R., and Mitchison, T.J. (2008). A novel small-molecule inhibitor reveals a possible role of kinesin-5 in anastral spindle-pole assembly. J. Cell Sci. *121*, 2293–2300.

Hentrich, C., and Surrey, T. (2010). Microtubule organization by the antagonistic mitotic motors kinesin-5 and kinesin-14. J. Cell Biol. *189*, 465–480.

Jaqaman, K., King, E.M., Amaro, A.C., Winter, J.R., Dorn, J.F., Elliott, H.L., Mchedlishvili, N., McClelland, S.E., Porter, I.M., Posch, M., et al. (2010). Kinetochore alignment within the metaphase plate is regulated by centromere stiffness and microtubule depolymerases. J. Cell Biol. *188*, 665–679.

Joglekar, A.P., and Hunt, A.J. (2002). A simple, mechanistic model for directional instability during mitotic chromosome movements. Biophys. J. *83*, 42–58.

Kapitein, L.C., Peterman, E.J.G., Kwok, B.H., Kim, J.H., Kapoor, T.M., and Schmidt, C.F. (2005). The bipolar mitotic kinesin Eg5 moves on both microtubules that it crosslinks. Nature *435*, 114–118.

Kapoor, T.M., and Mitchison, T.J. (2001). Eg5 is static in bipolar spindles relative to tubulin: evidence for a static spindle matrix. J. Cell Biol. *154*, 1125–1133.

Kashina, A.S., Baskin, R.J., Cole, D.G., Wedaman, K.P., Saxton, W.M., and Scholey, J.M. (1996). A bipolar kinesin. Nature *379*, 270–272.

Kitajima, T.S., Ohsugi, M., and Ellenberg, J. (2011). Complete kinetochore tracking reveals error-prone homologous chromosome biorientation in mammalian oocytes. Cell *146*, 568–581.

Ma, N., Titus, J., Gable, A., Ross, J.L., and Wadsworth, P. (2011). TPX2 regulates the localization and activity of Eg5 in the mammalian mitotic spindle. J. Cell Biol. *195*, 87–98.

Magidson, V., O'Connell, C.B., Lončarek, J., Paul, R., Mogilner, A., and Khodjakov, A.L. (2011). The spatial arrangement of chromosomes during prometaphase facilitates spindle assembly. Cell *146*, 555–567.

Maiato, H., Rieder, C.L., and Khodjakov, A.L. (2004). Kinetochore-driven formation of kinetochore fibers contributes to spindle assembly during animal mitosis. J. Cell Biol. *167*, 831–840.

Matos, I., Pereira, A.J., Lince-Faria, M., Cameron, L.A., Salmon, E.D., and Maiato, H. (2009). Synchronizing chromosome segregation by flux-dependent force equalization at kinetochores. J. Cell Biol. *186*, 11–26.

Mayer, T.U., Kapoor, T.M., Haggarty, S.J., King, R.W., Schreiber, S.L., and Mitchison, T.J. (1999). Small molecule inhibitor of mitotic spindle bipolarity identified in a phenotype-based screen. Science *286*, 971–974.

Mchedlishvili, N., Wieser, S., Holtackers, R., Mouysset, J., Belwal, M., Amaro, A.C., and Meraldi, P. (2012). Kinetochores accelerate centrosome separation to ensure faithful chromosome segregation. J. Cell Sci. *125*, 906–918.

McIntosh, J.R., Molodtsov, M.I., and Ataullakhanov, F.I. (2012). Biophysics of mitosis. Q. Rev. Biophys. *45*, 147–207.

Mountain, V., Simerly, C., Howard, L., Ando, A., Schatten, G., and Compton, D.A. (1999). The kinesin-related protein, HSET, opposes the activity of Eg5 and cross-links microtubules in the mammalian mitotic spindle. J. Cell Biol. *147*, 351–366.

Nicklas, R.B., and Arana, P. (1992). Evolution and the meaning of metaphase. J. Cell Sci. *102*, 681–690.

Nicklas, R.B., Kubai, D.F., and Hays, T.S. (1982). Spindle microtubules and their mechanical associations after micromanipulation in anaphase. J. Cell Biol. *95*, 91–104.

Press, W.H., Teukolsky, S.A., Vetterling, W.T., and Flannery, B.P. (2007). The Art of Scientific Computing, Third Edition. (New York: Cambridge University Press).

Qi, H., Rath, U., Wang, D., Xu, Y.-Z., Ding, Y., Zhang, W., Blacketer, M.J., Paddy, M.R., Girton, J., Johansen, J., and Johansen, K.M. (2004). Megator, an essential coiled-coil protein that localizes to the putative spindle matrix during mitosis in Drosophila. Mol. Biol. Cell *15*, 4854–4865.

Rieder, C.L., Davison, E.A., Jensen, L.C., Cassimeris, L., and Salmon, E.D. (1986). Oscillatory movements of monooriented chromosomes and their position relative to the spindle pole result from the ejection properties of the aster and half-spindle. J. Cell Biol. *103*, 581–591.

Samora, C.P., Mogessie, B., Conway, L., Ross, J.L., Straube, A., and McAinsh, A.D. (2011). MAP4 and CLASP1 operate as a safety mechanism to maintain a stable spindle position in mitosis. Nat. Cell Biol. *13*, 1040–1050.

Sawin, K.E., LeGuellec, K., Philippe, M., and Mitchison, T.J. (1992). Mitotic spindle organization by a plus-end-directed microtubule motor. Nature *359*, 540–543.

Shimamoto, Y., Maeda, Y.T., Ishiwata, S., Libchaber, A.J., and Kapoor, T.M. (2011). Insights into the micromechanical properties of the metaphase spindle. Cell *145*, 1062–1074.

Skibbens, R.V., Skeen, V.P., and Salmon, E.D. (1993). Directional instability of kinetochore motility during chromosome congression and segregation in mitotic newt lung cells: a push-pull mechanism. J. Cell Biol. *122*, 859–875.

Stumpff, J., Wagenbach, M., Franck, A.D., Asbury, C.L., and Wordeman, L. (2012). Kif18A and chromokinesins confine centromere movements via microtubule growth suppression and spatial control of kinetochore tension. Dev. Cell *22*, 1017–1029.

Sturgill, E.G., and Ohi, R. (2013). Kinesin-12 differentially affects spindle assembly depending on its microtubule substrate. Curr. Biol. *23*, 1280–1290.

Tanenbaum, M.E., Macůrek, L., Janssen, A., Geers, E.F., Alvarez-Fernández, M., and Medema, R.H. (2009). Kif15 cooperates with eg5 to promote bipolar spindle assembly. Curr. Biol. *19*, 1703–1711.

Tsai, M.-Y., Wang, S., Heidinger, J.M., Shumaker, D.K., Adam, S.A., Goldman, R.D., and Zheng, Y. (2006). A mitotic lamin B matrix induced by RanGTP required for spindle assembly. Science *311*, 1887–1893.

Vanneste, D., Takagi, M., Imamoto, N., and Vernos, I. (2009). The role of Hklp2 in the stabilization and maintenance of spindle bipolarity. Curr. Biol. *19*, 1712–1717.

Wandke, C., Barisic, M., Sigl, R., Rauch, V., Wolf, F., Amaro, A.C., Tan, C.H., Pereira, A.J., Kutay, U., Maiato, H., et al. (2012). Human chromokinesins promote chromosome congression and spindle microtubule dynamics during mitosis. J. Cell Biol. *198*, 847–863.

Waters, J.C., Mitchison, T.J., Rieder, C.L., and Salmon, E.D. (1996). The kinetochore microtubule minus-end disassembly associated with poleward flux produces a force that can do work. Mol. Biol. Cell *7*, 1547–1558.

Yamamoto, A., West, R.R., McIntosh, J.R., and Hiraoka, Y. (1999). A cytoplasmic dynein heavy chain is required for oscillatory nuclear movement of meiotic prophase and efficient meiotic recombination in fission yeast. J. Cell Biol. *145*, 1233–1249.